基于田口法的 PBGA 器件焊点可靠性分析

戴 玮, 薛松柏, 张 亮, 姬 峰
(南京航空航天大学 材料科学与技术学院, 南京 210016)

戴 玮

摘 要: 为提高塑料球栅阵列(PBGA)器件焊点可靠性, 提出了一种基于田口法和数值模拟的试验方法. 借用 Anand 模型描述钎料本构方程, 对 PBGA 器件焊点热循环载荷下的应力应变分布进行有限元模拟. 结果表明, 填充底充胶能有效提高焊点可靠性; 考虑基板、封装塑料、底充胶、PCB 的线膨胀系数四个控制因素, 借助田口试验法进行最佳参数选择, 确定影响焊点可靠性的主要因素为基板线膨胀系数及封装塑料线膨胀系数. 最优方案组合为 A3B3C3D3. 该优化方案的最大等效应变比原始值减小了 41.4%, 信噪比提高了 4.61 dB.

关键词: 塑料球栅阵列; 底充胶; 田口法; 线膨胀系数
中图分类号: TG40 文献标识码: A 文章编号: 0253-360X(2009)11-0081-04

0 序 言

由于重量轻、价格低廉等优点, 塑料球栅阵列器件(PBGA)在航空航天等领域有着广阔的应用前景. 但由于各组件之间线膨胀系数失配, 服役过程中功率的瞬间开、关引起的温度波动, 或者周围较复杂环境温度的改变, 都会导致 PBGA 焊点经受热循环并最终疲劳失效, 焊点的热疲劳损坏已经成为 PBGA 器件典型的失效方式[1].

为提高封装器件的可靠性, 研究者引入多种试验设计方法, 通过优化各组件的尺寸及材料性能来提高焊点的热疲劳寿命. Chiu 等人[2] 以焊点疲劳寿命为目标函数, 对焊点高度, 基板厚度等五个影响因素进行了因子设计. Zhou 等人[3] 结合人工神经元网络及粒子群算法, 研究了 PCB 大小及线膨胀系数(CTE)、芯片线膨胀系数、钎料球线膨胀系数等对 PBGA 焊点可靠性的影响. 此外, 还有研究者运用全面析因试验设计方法[4], 设计了芯片配重, 焊盘直径, 钢网厚度等多种不同工艺参数组合下的 PBGA 焊点可靠性.

田口法是一种低成本高效益的质量工程方法, 已有研究将其成功应用于焊点可靠性研究领域[5], 其核心分析工具是正交表和信噪比 $D_{S/N}$ (signal/noise), 以信噪比对由不同参数构成的产品实行功能性评价, 从中选择出最佳设计方案. 文中结合数值模拟技术和田口法, 以控制焊点非弹性应变范围为目标, 基于基板、封装塑料、底充胶、PCB 的线膨胀系数四个控制因素对填充底充胶的 PBGA 器件焊点热循环载荷下的可靠性进行研究.

收稿日期: 2009-05-14
基金项目: 2006 年江苏省"六大人才高峰"基金资助项目(06-E-020); 2009 年江苏省普通高校研究生科研创新计划资助项目(BCXJ09_07)

1 焊点可靠性有限元模拟

1.1 PBGA 有限元模型的构建

采用具有 208 颗焊球的 PBGA208 作为有限元计算的实体模型, PCB 尺寸为 12.16 mm×12.16 mm×1.524 mm, 焊球直径为 0.71 mm, 高度为 0.36 mm, 间距为 1.27 mm, BT 基板尺寸为 11.16 mm×11.16 mm×0.27 mm, 芯片尺寸为 3.81 mm×3.81 mm×0.5 mm.

将 PBGA 封装组件中硅芯片、封装塑料、基板、PCB 板均设为线弹性材料. 由于 Sn3.0Ag0.5Cu 钎料熔点为 223 ℃, 在服役过程中表现为粘塑性应力应变行为, 故常采用蠕变和塑性统一的 Anand 模型来描述钎料的力学本构关系, Anand 模型所需参数及钎料线性参数[6] 分别见表 1 和表 2. 有限元模型除焊点采用 Visco107 单元外, 其它组件均采用 Solid45 单元. 采取扫略划分方法划分网格. 网格划分结束后, 填充底充胶的模型共 33 134 个单元, 未填充底充胶的模型共 27 269 个单元. 填充底充胶时的模型网格划分结果及边界条件如图1所示. 按照美

表 1 Sn3.0Ag0.5Cu 钎料的 Anand 模型的粘塑性材料参数

Table 1 Visco-plastic parameters for Anand model

激活能 Q/(J·mol^{-1})	气体常数 R/(J·K^{-1}·mol^{-1})	常数 A/s^{-1}	应力乘子 ξ	敏感系数 m	系数 S/MPa	指数 n	硬化常数 h_0/MPa	应变指数 a	形变阻抗 S_0/MPa
62 022.4	8.314	5.87×10^6	2.0	0.094 2	58.3	0.015	9 350	1.50	45.9

国军用标准 MIL－STD－883，模型在－55～125 ℃进行温度循环加载，升温速率和降温速率均为 20 ℃/min，高温和低温的保温时间定为 25 min，有限元分析时采用三个温度循环周期进行计算.

表 2 线弹性材料参数

Table 2 Liner elastic material parameters

材料名称	弹性模量 E/GPa	泊松比 μ	线膨胀系数 α_l/(10^{-6}K^{-1})
Si 芯片	130.0	0.28	2.6
封装塑料	15.5	0.25	15.0
BT 基板	22.3	0.30	15.5
PCB	18.2	0.25	15.0
Sn3.0Ag0.5Cu	38.7	0.35	25.0
底充胶	11.0	0.30	21.0

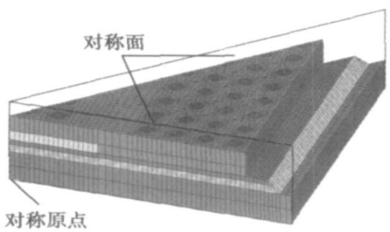

图 1 有限元模型及边界条件

Fig. 1 Finite element model and boundary conditions

1.2 有限元模拟结果

借助填充底充胶提高焊点热疲劳寿命，已经广泛应用于倒装芯片封装结构[7]. 尽管 PBGA 器件不填充底充胶也能得到较高的焊点热循环寿命，但还不能满足服役环境恶劣却对可靠性要求越来越高的航空航天等领域[8]. 填充底充胶进一步改善焊点可靠性，已成为 PBGA 可靠性的研究方向[9].

图 2a 为焊点阵列在不填充底充胶情况下的焊点应力分布. 明显可见应力集中区域在芯片下方焊点的上表面上，且应力最大位置出现在芯片拐角下方对应的焊球处. 填充底充胶后应力集中部位基本不变，但应力值明显减小，且应力均匀分布在芯片下方焊球的整个上表面，如图 2b 所示，并且填充底充胶后，应力值显著降低，对改善焊点的可靠性相当有益.

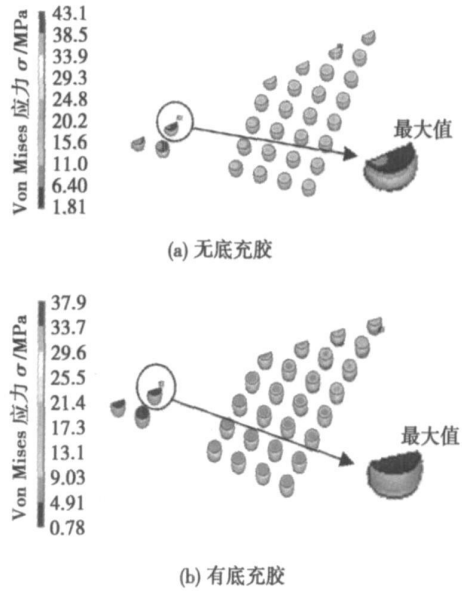

图 2 焊点应力云图

Fig. 2 Stress distributions of soldered joints

2 田口试验法

2.1 设计原理

田口法利用正交表安排试验，并将由损失函数引出的信噪比引入优化过程，得出不同影响因素对目标函数的影响程度，最后再通过验证试验确定优化结果的正确性. 利用正交表安排试验，可以减少模拟次数，并能得到可靠的试验数据.

由于各组件间的线膨胀系数不匹配是产生应力的主要原因，根据 PBGA 的结构组成，选定基板、封装塑料、底充胶、PCB 的线膨胀系数作为控制因素，每个因素取三个水平. 假设各因素间不存在相互作用，各材料参数如表 3 所示.

表 3 材料 CTE 水平配置

Table 3 Factors and levels of CTE

因素	材料	水平 1 α_{l1}/(10^{-6}K^{-1})	水平 2 α_{l2}/(10^{-6}K^{-1})	水平 3 α_{l3}/(10^{-6}K^{-1})
A	基板	15.5	18.5	21.1
B	封装塑料	15.1	13.8	11.6
C	底充胶	21.0	17.0	25.0
D	PCB	15.0	18.5	21.1

2.2　正交表构造及评价指标选择

采用正交表 $L_9(3^4)$ 安排试验，配置见表 3. 显然，该方案只需要进行 9 次试验，相比较全因子试验设计的 81 次，工作量已经大大减小.

选取焊点的非弹性应变范围 ΔE_p 作为评价焊点可靠性的评价指标，其值越小越不易被破坏. 要提高焊点可靠性，就要减小其非弹性应变范围.

2.3　信噪比分析

根据信噪比比值来评价评定指标（目标函数或多目标的评价函数）的优劣. 根据设计的目标特性（期望值越小越好），采用基于望小特性的 $D_{S/N}$ 公式为

$$D_{S/N}=-10\log\{\frac{1}{n}\sum_{i=1}^{n}y_i^2\} \qquad (1)$$

式中：n 为每一试验条件下的试验次数，文中采用的是数值模拟虚拟试验，因此 $n=1$；y_i 为试验值，文中为数值模拟得到的非弹性应变范围 ΔE_p 值.

数值模拟得到的评价指标值与其信噪比见表 4，表 5 为信噪比的平均效应响应，并表示在图 3 中. 从表 5 和图 3 中可以看出，对非弹性应变范围 ΔE_p 影响较大的因素为 A 基板 CTE 与 B 封装塑料 CTE. 同时还可以得到优化之后的最佳结构参数组合为 A3B3C3D3.

表 4　正交表构造及模拟结果

Table 4　Orthogonal array and test results

试验序号	影响因素及其水平				评价指标	信噪比
	A	B	C	D	非弹性应变范围 ΔE_p	$D_{S/N}$/dB
1	1	1	1	1	0.008 92	40.99
2	1	2	2	2	0.008 06	41.87
3	1	3	3	3	0.007 64	42.33
4	2	1	2	3	0.007 53	42.39
5	2	2	3	1	0.007 60	42.46
6	2	3	1	2	0.006 19	44.17
7	3	1	3	2	0.007 30	42.73
8	3	2	1	3	0.006 23	44.10
9	3	3	2	1	0.005 99	44.57
					均值	42.85

表 5　信噪比平均效应响应（dB）

Table 5　Average effect response for S/N ratio

	A	B	C	D
水平 1	41.73	42.04	43.09	42.68
水平 2	43.01	42.81	42.94	42.92
水平 3	43.80	43.69	43.44	42.94
效应	2.07	1.65	0.51	0.27
排名	1	2	3	4
最优	3	3	3	3

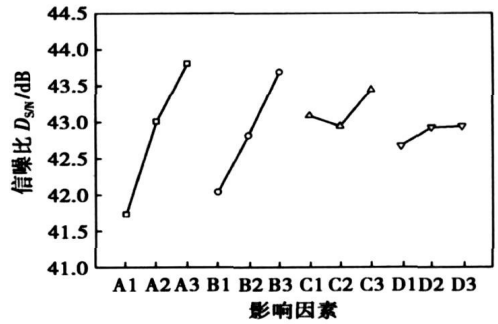

图 3　信噪比平均效应

Fig 3　Average effect diagram of S/N ratio

2.4　焊点可靠性的影响因素分析

田口方法采用 ANOVA（analysis of variance）评估正交试验中每个因素的响应量对评价指标的影响程度，使用各因素离差平方和分割总离差，计算每个因素的贡献率. 计算得出各个因素的贡献率如表 6 所示. 可以看到，影响因素 A，B，C，D 对 ΔE_p 的影响程度依次减小，且因素 A 基板 CTE 与因素 B 封装塑料 CET 对可靠性影响的贡献率之和达到 88.45%.

表 6　信噪比方差分析

Table 6　Analysis of variance for S/N ratio

因素	A	B	C	D
偏差平方和	2.20	1.37	0.42	0.04
贡献率（%）	54.60	33.85	10.45	1.10

2.4.1　基板 CTE 对焊点可靠性的影响

PBGA 基板在封装中起着机械支撑与电气连接的作用，由表 6 可见，其 CTE 即因素 A 对焊点可靠性影响显著. BT 材质的基板（CTE 为水平 A1）具有玻璃纤维纱层可以稳定尺寸，防止热胀冷缩而影响线路的良率，因此 BT 材质多用于对于可靠度要求较高的网络芯片及可程序逻辑芯片. 但是由于 BT 基板价格较高，发展其它类型较为廉价的基板如 FR5（CTE 为水平 A2），PPE（CTE 为水平 A3）能为制造商提供更多的选择. 由于所使用的钎料 Sn3.0Ag0.5Cu 的 CTE 为 2.5×10^{-5}/K，其与基板的 CTE 差异越小，焊点的可靠性越高. 若仅从基板材料 CTE 的角度来看，选用 FR5 及 PPE 也是可行的.

2.4.2　封装塑料 CTE 对焊点可靠性的影响

环氧树脂封装塑料（EMC）是 IC 后道封装三大主材料之一，用环氧树脂封装超大规模集成电路在国内外已成为主流. 由表 4 和图 3 可见，封装塑料的 CTE 越低，焊点可靠性越高. 此外，CTE 越小，在

封装过程中产生的应力越小，也不易产生翘曲、分层现象.

2.4.3 底充胶 CTE 对焊点可靠性的影响

当底充胶 CTE 为 2.5×10^{-5}/K 时，跟钎料的 CTE 相匹配，故焊点可靠性最高. 从表 6 可以看出，当填充胶的 CTE 为 1.7×10^{-5} ~2.5×10^{-5}/K 范围内，底充胶 CTE 对焊点可靠性的影响并不特别显著，故可以在一个较宽的范围内进行选择.

3 最优组合预测及验证

由图 3 可知，当选取最佳参数组合 A3B3C3D3 时，得到的 ΔE_p 最小，焊点的可靠性最高. 根据方差分析结果，基板 CTE 与封装塑料 CTE 对焊点等效应变范围 ΔE_p 影响较大，故仅考虑这两个因素对评价指标进行预估计. 原始设计的信噪比预估计计算公式为

$$D_{S/N}=D_{(S/N)\text{平均}}+[D_{(S/N)A1}-D_{(S/N)\text{平均}}]+[D_{(S/N)B1}-D_{(S/N)\text{平均}}] \quad (2)$$

最优设计信噪比的预估计计算公式为

$$D'_{S/N}=D_{(S/N)\text{平均}}+[D_{(S/N)A3}-D_{(S/N)\text{平均}}]+[D_{(S/N)B3}-D_{(S/N)\text{平均}}] \quad (3)$$

式中：$D_{(S/N)\text{平均}}$ 为 9 次模拟结果的信噪比均值；$D_{(S/N)A1}$ 为 A 因素在水平 1 条件下的信噪比值；$D_{(S/N)B1}$ 为 B 因素在水平 1 条件下的信噪比值；$D_{(S/N)A3}$ 为 A 因素在水平 3 条件下的信噪比值；$D_{(S/N)B3}$ 为 B 因素在水平 3 条件下的信噪比值. 预测结果及实测结果如表 7 所示，根据优化设计得到的非弹性应变范围 ΔE_p 比原始设计降低了 41.4%，信噪比提高了 4.61 dB.

表 7 优化结果与验证试验结果比较

Table 7 Comparison between experimental data and predictive value before and after optimization

	因素及水平				非弹性应变范围 ΔE_p	预测信噪比/dB	实测信噪比/dB
	A	B	C	D			
原始	1	1	1	1	0.008 92	40.80	40.99
最佳	3	3	3	3	0.005 24	44.64	45.61

4 结 论

(1) 填充底充胶后，芯片下方的焊球上表面应力均匀分布，PBGA 封装体在焊球处的应力集中程度减小，焊点可靠性提高.

(2) 结合田口法，利用正交表安排试验，提高了试验效率，得出影响焊点可靠性的主要因素为基板的 CTE 与封装塑料的 CTE，两者对可靠性影响的贡献率之和达到 88.45%.

(3) 经过优化设计，得到最优参数组合为 A3B3C3D3. 在此条件下进行试验，得到的非弹性应变范围 ΔE_p 比原始设计降低了 41.4%，信噪比提高了 4.61 dB.

参考文献：

[1] Arulvanan P, Zhong Z W. Assembly and reliability of PBGA packages on FR-4 PCBs with SnAgCu solder[J]. Microelectronic Engineering, 2006, 83(11-12): 2462-2468.

[2] Chiu C C, Wu C J, Peng C T, *et al*. Failure life prediction and factor design of lead-free flip chip package[J]. Journal of the Chinese Institute of Engineers, 2007, 30(3): 481-490.

[3] Zhou J C, Xiao X Q, En Y F, *et al*. Thermo-mechanical fatigue reliability optimization of PBGA solder joints based on ANN-PSO[J]. Journal of Central South University of Technology, 2008, 15(5): 689-693.

[4] 黄春跃，周德俭，吴兆华. 基于全面析因试验的塑封球栅阵列器件焊点可靠性[J]. 西安交通大学学报，2005，39(7)：753-756.
Huang Chunyue, Zhou Dejian, Wu Zhaohua. Solder joint reliability of plastic ball grid array component based on design of full factorial experiment[J]. Journal of Xi'an Jiaotong University, 2005, 39(7): 753-756.

[5] Jong W R, Tsai H C, Chang H T, *et al*. The effects of temperature cyclic loading on lead-free solder joints of wafer level chip scale package by Taguchi method[J]. Journal of Electronic Packaging, 2008, 130(3): 1-10.

[6] 张 亮，薛松柏，卢方焱，等. FCBGA 器件 SnAgCu 焊点疲劳寿命预测[J]. 焊接学报，2008，29(7)：85-88.
Zhang Liang, Xue Songbai, Lu Fangyan, *et al*. Fatigue life prediction of SnAgCu soldered joints of FCBGA device[J]. Transactions of the China Welding Institution, 2008, 29(7): 85-88.

[7] Wan J W, Zhang W J, Bergstrom D J. Recent advances in modeling the underfill process in flip-chip packaging[J]. Microelectronics Journal, 2007, 38(1): 67-75.

[8] Qi H, Osterman M, Pecht M. Plastic ball grid array solder joint reliability for avionics applications[J]. IEEE Transactions on Components and Packaging Technologies, 2007, 30(2): 242-247.

[9] Zhang L, Wang L, Xie X, *et al*. An investigation on thermal reliability of underfilled PBGA solder joints[J]. IEEE Transactions on Electronics Packaging Manufacturing, 2002, 25(4): 284-288.

作者简介：戴 玮，男，1986 年出生，硕士研究生. 主要从事微电子焊接及无铅钎料研究. 发表论文 3 篇.

Email：dave_d_w@126.com

Materials Science and Engineering, Shenyang University of Technology, Shenyang 110178, China). p 73—76

Abstract: The nickel-base alloy was deposited on the low carbon steel by plasma arc surfacing with transverse magnetic field. The influence of transverse alternative pulsed magnetic field frequency on microstructure and properties of plasma arc surfacing layer was researched. The hardness, wear resistance and microstructure of surfacing layer at different pulsed magnetic field currents were systematically analyzed by optical electronic microscope, wear test and microscopic hardness test. The results indicated that the transverse alternative pulsed magnetic field can effectively improve the crystal shape in plasma arc surfacing layer and refine crystal grain. With the proper pulsed magnetic field frequency, the optimum effect of electromagnetic stirring can be obtained, the amount of hardening phase in overlay deposit is increased, the growth direction of hardening phase can be controlled and the hardness and wear resistance of the surfacing overlay are improved.

Key words: plasma arc; transverse magnetic field; microstructure; wear resistance

3D reconstruction technology of SMT solder joint by shape from shading based on improved illumination model ZHAO Huihuang[1], ZHOU Dejian[2,3], HUANG Chunyue[3] (1. School of Mechanical and Electronical Engineering, Xidian University, Xi'an 710071, China; 2. Department of Mechanical Engineering, Guangxi University of Technology, Liuzhou 545006, Guangxi, China; 3. School of Mechanical and Electronical Engineering, Guilin University of Electronic Technology, Guilin 541004, Guangxi, China). p 77—80

Abstract: Three-dimensional shape and its accuracy are dissatisfactory because of the highlight caused by specular reflection when the shape from shading is used to reconstruct the three-dimensional soldered joint. An improved illumination model is proposed, which can modify the diffuse reflectance component based on the features of image shooting, make a linear superposition for both specular reflection component and diffuse reflectance component. Then the improved illumination model is used to reconstruct the three-dimensional soldered joint after dealing with the soldered joint image by the proper image processing arithmetic. The experimental results show that the 3D shape by SFS based on the improved illumination model is more satisfactory in decreasing specular reflection influence than that of the traditional methods.

Key words: surface mount technology; three-dimensional reconstruction; shape from shading; illumination model; image processing

Reliability analysis of PBGA soldered joints based on Taguchi method DAI Wei, XUE Songbai, ZHANG Liang, JI Feng (College of Materials Science and Technology, Nanjing University of Aeronautics and Astronautics, Nanjing 210016, China). p 81—84

Abstract: In order to evaluate the reliability of PBGA soldered joints, an optimized method was proposed based on Taguchi design and numerical simulation, in which the Anand equation was used to describe the viscoplastic behavior of Sn3.0Ag0.5Cu solder, and the distribution of equivalent stress and strain in soldered joints under temperature cycle were studied respectively. Results indicate that the thermal fatigue life of soldered joints can be substantially improved by filling up the underfill between the PCB and substrate. The linear expansion coefficients of substrate, epoxy mold compound, underfill and PCB were considered as the controlling factors, and the linear expansion coefficient of the substrate and that of epoxy mold compound were deemed to the main influencing factors by Taguchi method. The optimized controlling factor combination can be decided as A3B3C3D3, and the verification test shows the maximum equivalent strain of the optimization scheme was decreased by 41.4%, and the ratio of signal to noise was increased by 4.61 dB.

Key words: plastic ball grid array; underfill; Taguchi method; linear expansion coefficient

Contact reactive brazing between Al alloy/Cu/stainless steel and analysis on grain boundary penetration behaviors WU Mingfang[1,2], SI Naichao[1], PU Juan[2] (1. Jiangsu University, Zhenjiang 212013, Jiangsu, China; 2. Jiangsu University of Science and Technology, Zhenjiang 212003, Jiangsu, China). p 85—88

Abstract: Grain boundary penetration behavior occurs easily in the Al/Cu contact reactive brazing. In this paper, the mechanisms of formation and evolution of grain boundary penetration were investigated when contact reactive brazing between 6063 Al Alloy and 1Cr18Ni9Ti stainless steel was conducted using Cu as interlayer. The results show that the grain boundary penetration phenomenon is prominent. Grain boundary penetration depth was up to 200 μm when the brazing temperature was 570 ℃ and holding time was 60 min. The diffusion of atom into grain boundary was not sufficient but necessary for forming of grain boundary penetration. The key factor to induce grain boundary penetration was non-equilibrium diffusion of atom between the grain boundary and base metal, which led to crystal lattice expanding, and promoted the vacancy transferring into grain boundary, and resulted in a thin groove. And then, microcracks were formed in the grain boundaries, the eutectic liquid was sucked into the groove by capillary force, and finally grain boundary penetration was created. The interface reactive layer consisted of Fe-Al intermetallics (IMCs) in the side of 1Cr18Ni9Ti, the adjacent zone was Cu-Al IMCs, welded seam zone was composed of Al-Cu eutectic structure and large blocked Al solid solution.

Key words: Al Alloy; stainless steel; contact reactive brazing; grain boundary penetration; structure

Reaction mechanism and microstructure of interface in soldered joint of zinc based alloy LIU Xiuzhong[1,2], YANG Min[1,2], LIU Xinghong[3] (1. Key Laboratory of Liquid Structure and Heredity of Materials (Ministry of Education), Shandong University, Jinan 250061, China; 2. School of Materials Science and Engineering, Shandong University, Jinan 250061, China; 3. Xiangshan Tongjia Foundry-die Plant, Xiangshan 315700, Zhejiang, China). p 89—92

Abstract: The micro-region compositisions, fine microstructure and phases of interface region in joint soldered with new solder and flux self-developed were studied by means of XRD, EPMA, TEM and SEM. The results show that the interface region mainly consists of diffusion zone and dissolution zone. There was more Cd based solid solution (1.44% Zn) in diffusion zone, while more Zn based solid solution in dissolution zone. The interface region mainly consists of Cd, Sn, Zn, Al solid solution, and oxides such as SnO, SnO_2, CdO and metallic compounds such as MgZn, Mg_2Sn, Al_4Cu_9 and $Mg_2Cu_6Al_5$. No continuous intermetallic compounds layer which